



Published in final edited form as:

Prostate. 2013 April ; 73(5): 476–488. doi:10.1002/pros.22589.

Cathepsin D acts as an essential mediator to promote malignancy of benign prostatic epithelium

Freddie L. Pruitt¹, Yue He¹, Omar E. Franco², Ming Jiang², Justin M. Cates³, and Simon W. Hayward^{1,2,4}

¹Department of Cancer Biology, Vanderbilt University Medical Center, Nashville, TN

²Department of Urologic Surgery, Vanderbilt University Medical Center, Nashville, TN

³Department of Pathology, Vanderbilt University Medical Center, Nashville, TN

⁴Department of Vanderbilt-Ingram Cancer Center, Vanderbilt University Medical Center, Nashville, TN

Abstract

BACKGROUND—Stromal-epithelial interactions are important in both development and prostate cancer. Stromal changes have been shown to be powerful prognostic indicators of prostate cancer progression and of patient death helping to define lethal versus indolent phenotypes. The specific molecular underpinnings of these interactions are incompletely understood. We investigated whether stromal cathepsin D (CathD) overexpression affects prostate tumorigenesis through a paracrine mechanism.

METHODS—Normal prostate fibroblasts (NPF) were retrovirally transduced to overexpress cyclin D1 (CD1) cells were designated NPF^{CD1}. Cathepsin D expression was knocked down using shRNA in cancer associated fibroblasts (CAF) and NPF^{CD1}. We analyzed these stromal cell lines using immunohistochemistry, Western blot, and tissue recombination.

RESULTS—An examination of human prostate tissue revealed significantly increased stromal staining of CathD in malignant prostate tissue. Overexpression of CD1 in normal prostate fibroblasts (NPF^{CD1}) produced a phenotype similar to, but more moderate than, CAF in a tissue recombination model. Knockdown studies revealed that CathD is required for NPF^{CD1} motility and invasive growth *in vitro*. BPH-1 cell proliferation was found to be induced when cultured with NPF^{CD1} conditioned medium, this effect was inhibited when CathD was knocked down in NPF^{CD1} cells. Overexpression of CathD in prostate stromal cells induced malignancy in adjacent epithelium, and this transformation was inhibited when stromal CathD expression was knocked down in CAF.

CONCLUSIONS—The study presented here demonstrates increased CathD expression is seen in human CAF. The upregulation of CD1 results in concomitant increases in CathD expression. Elevated CathD expression in the stroma contributes to tumor promotion.

Keywords

cathepsin D; stromal-epithelial interactions; prostate cancer

Introduction

Historically, the field of cancer biology has primarily been focused on studying the malignant tumor epithelium [1]. The emergence of the field of tumor microenvironment is providing some much needed insight into how non-malignant cells associated with cancer (cancer associated stroma) can promote or suppress tumorigenesis. The stromal phenotype has been shown to be a powerful prognostic indicator of cancer progression and of patient death underlining the importance of local stromal cells in defining lethal versus indolent phenotypes [2].

Stromal-epithelial interactions are important in both the development of the prostate, and in prostate cancer (PCa) [3–5]. During carcinoma evolution, the stroma cells adjacent to the pre-malignant or malignant epithelium experience phenotypic alterations that have been shown to enhance the invasive potential of the epithelial tumor [6–8]. These stromal-epithelial interactions are mediated, in large part, by paracrine signaling between epithelial tumor cells and neighboring stromal fibroblasts [8]. We have previously published on several molecules found to be aberrantly expressed in cancer associated stroma that induce tumorigenesis and malignant conversion [7–13]. These intercellular interactions are clearly complex and there are likely a number of molecular routes which can either promote or suppress tumor-inducing activity. One purpose of pursuing these studies is to start to determine the identity of pathways which are either sufficient or necessary to induce transformation and to examine how such pathways might interact. We showed that the up-regulation of a cell cycle regulator known as cyclin D1 (CD1) in normal prostate fibroblasts mimics aspects of the phenotype of malignant conversion seen in cancer associated stroma. In addition to receiving signals from malignant epithelial cells, the stromal fibroblasts stimulate tumorigenesis by releasing factors that act on adjacent epithelial tumor cells or exchange enzymes that modify local microenvironment promoting the proliferation and survival of the neoplastic cells [7, 8, 14, 15].

One mechanism by which modifications to the local tumor microenvironment are accomplished is via the actions of several different families of proteases produced by either the tumor or the stroma [16]. These enzyme families include matrix metalloproteases (MMP), cysteine, and serine proteases, which have been shown to play a role in the degradation of the basement matrix, promotion of angiogenesis, and the liberation of growth factors to stimulate tumor cell growth [17, 18].

Cathepsin D (CathD) is a ubiquitous lysosomal aspartic endoproteinase. CathD, has been shown to be involved in a number of physiological processes, playing a critical role in barrier function, regulation of apoptosis, and epithelial differentiation [19–21]. In cancer, CathD is overexpressed and hypersecreted in various malignancies including PCa [22, 23]. In breast cancer, CathD expression is associated with a poor prognosis and increased likelihood for the development of metastasis [24]. Experimental evidence has shown CathD can stimulate the proliferation of PCa cell lines [25].

There are limited data defining CathD's function in prostate cancer progression. Some studies have concluded that CathD is overexpressed in the epithelium and stroma of PCa, and may promote proliferation [25, 26]. Other studies have concluded that CathD produced by PCa may be inhibiting tumor growth [27, 28]. In the present study, we highlight CathD as a mediator of cancer associated stromal promotion of prostate tumorigenesis.

Methods

Cells

BPH-1 (a non-tumorigenic human prostatic epithelial cell), and its tumorigenic derivatives BPH^{CAFTD} were from our own stocks [29, 30]. CAF cells were isolated from human prostate tumor samples and their activity validated in a tissue recombination model. The technique for the isolation of CAF is described in Olumi et al. [4] which also describes a bioassay which was used to confirm the tumor-inducing activity of the CAF used in the present study. NPF^{CD1} cells, which we have shown in the past to overexpress CathD, were generated as previously described [9]. Benign human prostate stromal cells (BHPPrS1) were isolated from a prostate surgical sample and immortalized with hTERT as previously described [10]. Cells were maintained in RPMI 1640 (Gibco, Carlsbad, CA) with 1% antibiotic/antimycotic (Life Technologies, Grand Island, NY) and 5% Cosmic Calf Serum (CCS-HyClone, Logan, Utah).

Generating genetically modified cell lines

The pSuper.Retro-control (PSR-OligoEngine, Seattle, WA) and pSuper.Retro-CD1 shRNA (PSR-CD1sh) were kindly provided by Drs. Rene Bernards and Daniel Peeper from the Netherlands Cancer Institute. The two plasmids were engineered into CAF by retroviral transduction as previously described [9]. Positively transduced cells were selected for resistance to puromycin (5 μ g/ml) to generate two cell strains (CAF^{scram} and CAF^{CD1sh}). The pSilencer 2.1-CathD1shRNA vector was kindly provided by Dr. Daniel E. Johnson from the University of Pittsburgh Cancer Institute. PSR-cathepsin Dsh was generated by removing the CathD1sh coding sequence from pSilencer 2.1-CathD1shRNA with HindIII and BamHI and ligated into the PSR construct. The PSR and PSR-CathD sh were engineered into CAF by retroviral infection as described previously [9]. The positive transduced cells were selected for resistance to puromycin (5 μ g/ml) to generate the cell line (CAF^{CathDsh}). BPH-1^{NPF}, BPH-1^{CAFTD1}, and BPH-1^{NPFCD1} cells were re-isolated from resulting growths as previously described [9]. BHPPrS1 cells were engineered to overexpress CathD by lentiviral transduction (Genecopoeia Inc, Rockville, MD.) Viral supernatant was generated, centrifuged at 3000 rpm for 5 min and passed through a 0.45 μ m filter before frozen at -80°C until used. Polybrene (Sigma-Aldrich, St Louis, MO) was added to the viral suspension at 5 μ g/mL to increase the efficiency of the transduction. GFP-expressing cells were selected by fluorescence-activated cell sorting (FACS) to establish the BHPPrS^{CathD} and BHPPrS^{EV} as an empty vector control.

Western blotting analysis

Cell lysates were prepared and Western blotting was performed as previously described [31]. Membranes were incubated with mouse primary antibody to PTEN (1;1000, Santa Cruz Biotechnology, Santa Cruz, CA), Cdk2 (1;1000, Santa Cruz), Cdk4 (1;1000, Santa Cruz), Cdk6 (1;1000, Santa Cruz), cyclin E (1:1000, Santa Cruz), CD1 (1:1000, BD Biosciences Pharmingen, San Jose, CA), β -actin (1:5000, Sigma) or CathD (1:1000, Cell Signaling, Denvers, MA) overnight and washed with PBS-Tween 20 for 1 hour, and incubated with horseradish-Peroxidase linked anti-mouse secondary antibody (Amersham Biosciences, Piscataway, NJ, 1:10,000 dilution) for 1 hour. Bound antibodies were visualized using enhanced chemiluminescence western blotting detection reagents (Amersham Biosciences).

Tissue recombination and xenografting

Rat urogenital mesenchyme (rUGM) was obtained from 18-day embryonic fetuses (plug date denoted as day 0). Urogenital sinuses were dissected from fetuses and separated into

epithelial and mesenchymal components by tryptic digestion, as described previously [32]. BPH-1 + rUGM, BPH-1 + NPF, BPH-1 + NPF^{CD1}, BPH + CAF, BPH-1 + CAF^{CyclinD1sh}, BPH-1 + CAF^{CathDsh}, BPH-1 + BHP^{rS}^{CathD}, and BPH-1 + BHP^{rS}^{EV} tissue recombinants were made as previously described [33]. 1.0×10^5 epithelial cells and 2.5×10^5 stromal cells combined in type I rat tail collagen were used to make the recombinants. After overnight incubation, the tissue recombinants were grafted under the kidney capsule of adult male severe combined immunodeficient (SCID) mice (Harlan, Indianapolis, IN) supplemented with 25mg testosterone pellets (PCCA, Houston TX). All the experiments were repeated six times. Mice were sacrificed at eight weeks and grafts were harvested, fixed, and paraffin embedded. Graft dimensions were measured using the formula: volume = width \times length \times depth $\times \pi/6$ as described previously [10].

Wound healing assays

Confluent monolayers of NPF and NPF^{CD1} cells were grown in 6 well plates. Confluent cell monolayers were wounded by scratching with a pipette tip. Specific points on the wounds were identified and marked. These open areas were then inspected microscopically over time as the cells migrated in and fill the damaged area. Wounds were imaged at 0, 3, 6, and 8 hours post wounding and the cell migration rate into the wound was calculated. Experiments were performed in triplicate.

Outgrowth assay

1.0×10^5 NPF, NPF^{CD1}, NPF^{CD1}-CathD control or NPF^{CD1}-CathDsh were resuspended at 4°C in Matrigel (0.2 ml, 10 mg/ml; Becton and Dickinson), and overlaid to a previously solidified layer of Matrigel in 24-well plates as described previously. The top Matrigel layer was solidified at 37°C for 30 minutes and covered with culture medium containing 10% FCS (0.5 ml).

Conditioned Medium

NPF or NPF^{CD1} were seeded with 5% FCS in RPMI 1640 at a density of 5.0×10^5 per 75-cm² flask, allowed to grow, and attached overnight. Confluent cultures of NPF or NPF^{CD1} were rinsed twice in PBS and incubated for 3 days in RPMI + 0.5% FCS. The medium was collected, centrifuged, passed through a 0.45- μ m filter (Millipore), and stored at -80°C for later use. Conditioned medium was thawed and diluted 1:1 with fresh DMEM + 0.5% FCS before use. BPH-1 cells were seeded at 2.0×10^4 per well in six-well plates in conditioned medium. The cultures were incubated for 3 days and the total number of cells was determined by direct counting in a hemacytometer.

Human Prostate and Prostate Tissue Microarray

Human prostate tissue array (PR806) was obtained from US Biomax, Inc. The array contained duplicates from 30 cases of adenocarcinoma ranging in Gleason scores and 10 cases of normal prostate tissue. Normal human prostate tissue was also obtained from the Vanderbilt University Medical Center Department of Pathology.

Histochemical and Immunohistochemical staining

Masson's trichrome stain was performed as previously described using Diagnostics Accustain Masson trichrome stain kit (Sigma), Bouin's solution (Sigma) and Weigert's Iron Hematoxylin set (Sigma) [10]. Immunohistochemical staining was performed following a protocol that was described previously [31]. Tissue slides were then incubated with the primary antibody against CD1 (1:200, BD Biosciences Pharmingen), CathD (1:200, Santa Cruz), p-SMAD2/3 (1:400, Santa Cruz), Col4A2 (1:200, Santa Cruz), The polyclonal rabbit or mouse immunoglobulins/biotinylated anti-mouse secondary antibody (DAKO,

Carpentiria, CA) was incubated for 60 min after the slides were washed with PBS buffer for 1 hour. After washing the slides in PBS extensively, slides were incubated in ABC-HRP complex (Vector Laboratories) for 30 minutes. Bound antibodies were then visualized by incubation with 3,3'-diaminobenzidine tetrahydrochloride (liquid DAB, DAKO). Slides were then rinsed extensively in tap water, counterstained with hematoxylin, and mounted.

Immunofluorescence

For histological analysis, 5 μ m tissue sections were dewaxed, and the antigen was unmasked by heating samples in unmasking solution (Vector Laboratories). Slides were blocked in 12% BSA in PBS for 30 minutes at room temperature before incubating with primary antibodies against CathD and GFP (1:200, Santa Cruz). After 1 hour washing in PBS buffer, slides were incubated with secondary antibodies (1:200; AlexaFlour 488 anti-Rabbit IgG and AlexaFlour 594 anti-mouse IgG2a) for 30 minutes at room temperature. Slides were incubated in Hoechst 33258 (4mg/L) for 5 min. Tissue sections were washed for 30 minutes in PBS, mounted, and visualized.

Quantitative Image Analysis

Immunostained slides were analyzed using the Ariol SL-50 automated slide scanner (Applied Imaging, San Jose, CA) to quantitate the amount of staining for CathD in the stroma of benign and malignant human prostate tissue sections. Positive staining was calculated by applying 2 thresholds, with one recognizing weaker brown-positive cells, and another recognizing stronger brown-positive cells. The intensity of the stain was calculated by masking out all non-stromal areas from the tissue section and calculating the integrated optical density of brown within the remaining area. This value was divided by the area in pixels of the brown mask to calculate the average intensity of the tissue section.

Statistical Analysis

Data from *in vitro* and *in vivo* are presented as the mean \pm standard deviation (SD). The data was analyzed using GraphPad PRISM software (La Jolla, CA). P values less than .05 were considered statistically significant. Quantitated intensity of CathD expression in human prostate samples were compared with analysis of variance followed by post hoc analysis of significant means by Mann Whitney's test was used in comparison of normal to tumor tissue. Post hoc analysis of significant means by Dunn's Multiple Comparison test was used for the comparisons of normal tissue with low grade and high grade malignant prostate tissue. P values less than .05 were considered statistically significant.

Results

CathD expression is upregulated in prostate clinical samples, and CathD is overexpressed in the stroma of tumorigenic tissue recombinants

We examined the expression patterns of CathD in human prostate clinical samples using a tissue microarray containing 30 cases of adenocarcinoma, 10 cases of normal prostate tissue. The tissue microarray contained duplicate cores per case. Quantification of positive CathD staining in stromal regions of prostate tissue showed significantly greater areas of CathD expression in tumor tissue in comparison to normal prostate tissue. When tumor tissue was stratified between low and high grades, a significant difference was only observed in high grade tumors compared with normal tissue with a non-significant elevation of expression in low grade tumors (Figure 1). A similar trend with no significant difference was also observed in comparisons of low and high grade tumors. It was noteworthy that the expression of CathD apparently corresponded to areas, which stained a light red color in the adjacent trichrome-stained sections. This likely indicates the presence of myofibroblastic

cells in this area, which would correspond to the source of our experimental CAF. Examination of CathD expression in tissue recombinations of BPH-1+NPF, BPH-1+rUGM, BPH-1+NPF^{CD1}, and BPH-1+CAF was performed by IHC. The recombinations of BPH-1 + NPF and BPH-1 + UGM isolated after 8 weeks of growth produced small growths overall which displayed solid epithelial cord structures surrounded by a muscular stroma. IHC staining displayed minimal expression of CathD in the stroma with some epithelial expression seen in the BPH-1 + NPF recombinants (Figure 2A, 1 and 2A, 2). In marked contrast, recombinations of BPH-1 + NPF^{CD1} and BPH-1 + CAF isolated after 8 weeks produced poorly differentiated carcinoma along with areas of squamous metaplasia similar to previously published results (Figure 2A, 3 and 2A, 4) [9]. Recombinations of BPH-1 + NPF^{CD1} and BPH-1 + CAF displayed strong CathD staining in the stroma and epithelium (Figure 2A, 3 and 2A, 4). These results are consistent with the observations of CathD overexpression in the stroma of human PCa clinical tissues. These data raised the question of whether the upregulation of CathD protein is a passive result of prostatic tumorigenesis or plays an active role as a paracrine mediator required to induce a malignant transformation in the adjacent prostatic epithelium.

Stromal expression of CD1 affects cell cycle regulators in adjacent epithelium

Fluorescence-activated cell sorting of BPH-1 cells isolated from the xenografts of BPH-1 + NPF, and BPH-1 + NPF^{CD1} tissue recombinants showed striking differences in cell population distributions. Previously published DNA flow cytometric analysis showed a majority (55%) of BPH-1 cells isolated from the tissue xenografts of BPH-1 + NPF^{CD1} were hyperploid along with another large population of BPH-1 cells (23.1%) that were polyploid [9]. In order to gain some insight as to what signaling pathways in BPH-1 cells were being affected by NPF^{CD1} we performed western blot analysis for several proteins involved in cell cycle regulation. Epithelial cells were isolated and cultured from xenografts of BPH-1+NPF, BPH-1+CAF and BPH-1+NPF^{CD1}. The resulting cells were designated BPH-1^{NPF}, BPH-1^{CAFTD} and BPH-1^{NPF-CD1} respectively. Densitometric analysis of band intensities from western blots revealed that overexpression of CD1 in the local stromal cells increased the expression of the cell cycle related proteins CD1, cyclin dependent kinases-6 (CDK6) and 2 (CDK2), and CathD in BPH-1^{NPF-CD1} over BPH-1^{NPF} (Figure 2B), consistent with increasing proliferative activity in these cells. Similar results were observed in BPH-1^{CAFTD}. No changes in the expression CDK4, cyclin E were observed.

CathD is a critical component in NPF^{CD1} motility and 3D outgrowth

We have previously reported the abilities of NPF^{CD1} and CAF to induce tumorigenesis in tissue recombination experiments [4, 9]. In order to further investigate mechanisms underlying this malignant transformation we characterized the effects of knocking down CathD expression in NPF^{CD1}. NPF^{CD1} displayed enhanced motility in wound healing assays compared with control NPFs (Figure 3A). The enhanced motility displayed by NPF^{CD1} was significantly abrogated when CathD expression was knocked down, with the use of CathD specific shRNA (NPF^{CD1}-CathDsh) (p-value<0.005). These findings demonstrate that CathD plays a role in NPF^{CD1} migration *in vitro*. Western blot analysis was performed to confirm the knockdown of CathD expression in CD1 overexpressing fibroblast (Figure 3D). Overexpression of CD1 in NPF results in increased CathD expression as previously published [9]. Stable expression of stable hairpin RNA (shRNA) specific for CathD results in 66% knockdown in CathD expression. Expression of non-specific shRNA in NPF^{CD1} does not alter CathD expression.

To further characterize the requirement for CathD expression in NPF^{CD1}, we examined fibroblast outgrowth in 3D matrices. As shown in Figure 3B, overexpression of CD1 promoted outgrowth of normal prostatic fibroblasts embedded into Matrigel. After 14 days

of culture, NPF^{CD1} cells had adopted a stellate morphology and formed invasive colonies with protrusions sprouting into the surrounding matrix (Figure 3N, 2). In contrast, normal prostatic fibroblasts presented a well-delineated spherical appearance of quiescent and/or dying cells and grew poorly, neither invading nor forming protrusions to the surrounding matrix (Figure 3B, 1). NPF^{CD1-CathD^{sh}} cultured in 3D matrix failed to form invasive colonies that protruded into the surrounding matrix (Figure 3B, 3), unlike NPF^{CD1-control}, which retained the ability to form invasive growth feature (Figure 3B, 4). These data strongly imply a role for CathD as a factor in promoting the invasive growth of NPF^{CD1} cells *in vitro*.

CathD is a paracrine mediator of neoplastic epithelial cell growth *in vitro*

To investigate the role of CathD as a paracrine mediator of prostate epithelial cell growth, we generated conditioned media from NPF and NPF^{CD1} cells, and measured BPH-1 cell numbers after growth for three days in the conditioned media. Conditioned medium from NPF^{CD1} increased the proliferation of BPH-1 cells by 1.7-fold, when compared with medium conditioned by parental NPF (Figure 3C). The pro-mitogenic effects from NPF^{CD1} conditioned medium were abrogated when CathD expression was knocked down in NPF^{CD1-CathD^{sh}} (p-value = 0.005). These results suggest that a significant component of NPF^{CD1} proliferative influence toward epithelium is mediated through secreted CathD.

CathD is an essential mediator of CAF induced tumorigenicity *in vivo*

To elucidate the role of CD1 and CathD in CAF's ability to induce tumorigenesis of BPH-1, we took a knockdown expression approach. CAF were engineered to express shRNA vectors specific for either CD1 or CathD. Western blotting was used to assess knockdown efficiency. CD1 expression was knocked down 50% and CathD expression was knocked down 95% in CAF cells (Figure 4C). Based on gross morphology it was found that BPH-1+CAF^{CyclinD1^{sh}} and BPH-1+CAF^{CathD^{sh}} recombinants formed significantly smaller grafts compared with BPH-1+CAF grafts (p-value = 0.05) (Figure 4A and C). Histologically, BPH-1+CAF recombinants formed adenosquamous carcinoma as previously described [4]. Knockdown recombinants formed benign, small cords structure with no tumorigenic response (Figure 4B). These findings establish CathD to be key mediators in prostate stroma-epithelial interaction in the development of tumorigenesis.

To further clarify the role of stromal derived CathD in promoting tumorigenesis we engineered BHPrS, a benign human prostate stromal cell line, to overexpress CathD (BHPrS^{CathD}) by lentiviral transduction. In comparison to recombinations of BPH-1 + BHPrS^{EV}, BPH-1 + BHPrS^{CathD} recombinants exhibited a malignant transformation. Based on the H&E staining recombinations of BPH-1 + BHPrS^{EV} exhibited thick stromal regions delineating BPH-1 cells from the kidney interface (Figure 5A). The opposite was observed in recombinations of BPH-1 + BHPrS^{CathD}, where BPH-1 cells are directly adjacent to kidney interface (Figure 5D). IHC staining for CathD indicates strong stromal expression of CathD in the recombinations of BPH-1 + BHPrS^{CathD} (Figure 5E). IF staining for GFP positive stromal cells (red) and CathD expression (green) show strong stromal specific expression of CathD seen in the yellow overlay (Figure 5F).

Masson's trichrome staining was performed on tissue sections from recombinations of BPH-1 + BHPrS^{EV} and BPH-1 + BHPrS^{CathD} (Figure 5G+5J). Heavy aniline blue stains indicated increased deposition of newly synthesized collagen fibrils in the CathD overexpressing recombinations (Figure 5J). IHC staining was performed to examine the phosphorylated-SMAD2/3 (p-SMAD2/3), a surrogate reporter of transforming growth factor-beta (TGF-β) activity (Figure 5H+5K). CathD overexpressing recombinations (Figure 5K) shows increased nuclear p-SMAD2/3 staining. Quantitation of p-SMAD2/3 positive

cells indicated a significant difference in the CathD overexpressing recombinations. Type IV ± 2 collagen (Col.IV ± 2) is a known TGF- β responsive gene. We performed IHC staining for Col.IV ± 2 and the CathD overexpressing recombinations (Figure 5L) displayed strong expression for Col.IV ± 2 in comparison to recombinations with the empty vector construct (Figure 5I).

Discussion

Tumor stroma has been implicated in the regulation of cell growth, determining metastatic potential, and impacting the outcome of therapy. Stromal-epithelial interactions in cancer have been implicated as promoting several malignancies including prostate, breast, colon, and pancreatic cancers [1, 4]. The stroma is often radically changed around malignant tumors and such changes both predict prognosis and may actually contribute to disease progression [1, 4]. We have previously examined the role of several molecules found to be aberrantly expressed in cancer associated stroma that induce tumorigenesis and malignant conversion [8]. We reported that CD1-overexpressing BPH-1 cells are non-tumorigenic in the presence of rUGM in tissue recombination experiments, but in contrast, the overexpression of CD1 in prostate fibroblasts induces a strong tumorigenic response in the non-malignant but genetically initiated BPH-1 cells [9]. The tumor-promoting abilities of NPF^{CD1} produce changes very similar to published descriptions of tissue recombinations of CAF with BPH-1 [4]. A comparison of the genetic profiles from CAF and NPF^{CD1} identified CathD as being upregulated 7-fold in comparison to NPF [9]. From this finding we hypothesized that CathD may be a mediator of stromal-epithelial interactions contributing to prostate tumorigenesis.

CathD overexpression in neoplastic cells and neoplasia-associated connective tissue was described as long as 24 years ago, and is reported to play several roles in cancer progression [34–37]. Cathepsins have recently been shown to be upregulated in a pancreatic tumor model and also contribute to invasive breast tumor growth [38–40]. We previously reported that CathD is upregulated in both NPF^{CD1} cells (which mimic CAF) as well in CAF. Microarray analysis revealed a 7-fold increase in CathD resulting from CD1 expression in NPF. NPF^{CD1} cells display increased motility in comparison to control NPFs in a wound healing assay which was shown to depend upon the expression of CathD [9]. Here we show that the ability of NPF^{CD1} to survive and invade into 3D matrices was also dependent on CathD. The overexpression of CD1 in NPF produced invasive colonies with protrusions sprouting into the surrounding matrix. This invasive growth was inhibited in NPF^{CD1} cells when CathD expression was knocked down. This finding is supported by similar results from Laurent-Matha et al. where CathD was critical for outgrowth of human fibroblast in 3D matrices. [22]. Our findings were consistent with a model in which CD1-induced overexpression of CathD resulting in increased fibroblast motility and invasion.

An immunohistochemical examination of clinical specimens revealed low levels of expression of CathD in normal prostate stromal tissue. Malignant areas showed prominent stromal expression of CathD, with the significantly greater stromal CathD expression in high grade tumor samples. IHC analysis of CathD expression in tissue recombinations of BPH-1+CAF and NPF^{CD1} also revealed strong stromal staining in comparison to recombinations of BPH-1+NPF and BPH-1+rUGM. CathD expression in human prostate cancer stroma correlates, with shorter survival and recurrence-free periods [41]. Our experimental data establishing a link between the overexpression of CD1 with the up-regulation of CathD in prostate CAF, coupled with the similar findings in human disease indicates a strong association between cell cycle regulation and protease expression in prostate tumorigenesis. The cell cycle regulator CD1 and the estrogen receptor alpha (ER \pm) are known to interact and can induce estrogenic gene transcription [42]. This suggests the

possibility that the overexpression of CathD in PCa associated stroma is due to the interaction of ER \pm with CD1.

Further investigation into the role of CathD in the tumor microenvironment showed that CathD expression is necessary for NPF^{CD1} cells to promote epithelial growth under *in vitro* conditions. The pro-mitogenic effect of NPF^{CD1} conditioned medium on BPH-1 cells was inhibited when CathD expression was knocked-down in NPF^{CD1}. This result mirrors published findings showing that CathD is mitogenic to PCa cell lines [25]. These data do not, of course, imply that CathD is a direct mitogen, merely that its presence results in a mitogenic environment. Given the possibility that this protease may activate latent growth factors associated with extracellular proteoglycans an indirect mechanism is not only possible but likely.

To further pursue an underlying mechanism we engineered BHP_rS cells to overexpress CathD and combined these BHP_rS^{CathD} cells with BPH-1 and performed renal grafting experiments. Recombinations of BPH-1 cells with BHP_rS resulted in benign solid epithelial cords similar to recombinations of NPF with BPH-1 cells [10]. However, the overexpression of CathD in BHP_rS in recombination experiments with BPH-1 cells induced a malignant transformation with invasion into the mouse kidney. This is consistent with our findings with the CathD knockdown approach in experiments with the CAFs. A feature of the prostate tumor microenvironment in human disease is the expansion of myofibroblast like cells with increased deposition of extracellular matrix proteins [18]. Masson's trichrome staining of tissue xenografts from the CathD overexpressing stromal cells revealed increased production of collagen in comparison to recombinations with the EV control stromal cells. These staining patterns were similar to previous publications that pointed towards altered TGF- β signaling. We have previously shown that the overexpression of TGF- β in BHP_rS cells resulted in the development of poorly differentiated adenocarcinoma with increased deposition of collagen in tissue recombination experiments [10]. TGF- β is expressed by most cultured cells in an inactive form due to binding with latent complex, and activation requires the proteolytic degradation of this complex. CathD derived from fibroblast conditioned media has been shown to liberate active TGF- β from the latent complex [43]. Investigation of altered TGF- β signaling in our model revealed increased p-SMAD2/3 staining, a surrogate marker for TGF- β response, in the CathD overexpressing recombinations. Examination of Col.IV \pm 2, a direct TGF- β responsive gene, expression in the tissue xenografts revealed increased staining for Col.IV \pm 2. Collectively, the differences in stromal composition observed from trichrome staining can be linked to increased TGF- β signaling and responsive gene expression as a result of stromal derived CathD. The overexpression of CathD in the stroma resulted in a somewhat minor, all though sufficient, malignant transformation of initiated epithelial cells similar to the tumor inductive properties of CAF.

We previously demonstrated that NPF^{CD1} cells and CAF elicited permanent malignant transformation of BPH-1 cells [9, 30, 44]. Data from IHC of clinical tissue showed increased CathD in the stroma adjacent to malignant regions of the prostate. To address the contribution of CathD in CAF-induced tumorigenesis of BPH-1, we engineered CathD knock-down CAF. The ability of CAF to induce tumorigenesis in BPH-1 recombinations was abolished when CathD expression was knocked-down. Similar results were observed when CD1 expression was knocked down in CAF. These data indicated that CathD is not only an important mediator of stroma-epithelial cross talk *in vitro*, but also an essential component in promotion of tumorigenesis *in vivo*, at least in this model.

In summary, the study presented here demonstrates that CathD can play a role as a paracrine mediator contributing to prostate tumorigenesis. The identification of key players, such as

CathD, that participate in the promotion of the tumor microenvironment contributes to our understanding of the molecular mechanisms underlying this process and may prove to be valuable for the development of novel anti-cancer therapies. Current anti-cancer therapies target the malignant epithelial cells, which progressively acquire genetic alterations during the progression of the disease [45–47]. The biggest obstacle facing clinicians treating people with cancer in general is the toxicity of treatments combined with the development of resistance to therapy. The tumor microenvironment has been shown to be more genetically stable and therefore less likely to develop resistance to novel anti-cancer therapeutics [48, 49]. Since tumor promotion by the microenvironment is a function of many different signaling molecules it should be possible to develop therapeutic strategies which appropriately modify several pathways simultaneously rather than simply attempting to totally block a single signal. This is likely to be both more effective and better tolerated, since the normal biological effects of the molecules concerned will be less affected. Further investigation is needed to explain in detail how CathD is acting. A better understanding of the complexities of CathD in the tumor microenvironment may provide targets for suppressing lethal PCa phenotypes.

Acknowledgments

Grant Acknowledgments: This work was funded by the taxpayers of the United States via NIH grant U01 CA151924 (SWH), and DOD-PCRP predoctoral fellowships W81XWH-07-1-0139 (YH) and W81XWH-01-1-0328 (FP).

References

- Weinberg RA. Coevolution in the tumor microenvironment. *Nat Genet.* 2008; 40:494–495. [PubMed: 18443582]
- Li H, Fan X. Tumor microenvironment: the role of the tumor stroma in cancer. *Journal of cellular biochemistry.* 2007
- Cunha G. Tissue interactions between epithelium and mesenchyme of urogenital and integumental origin. *The Anatomical Record.* 1972
- Olumi A, Grossfeld G, Hayward S, Carroll P. Carcinoma-associated fibroblasts direct tumor progression of initiated human prostatic epithelium. *Cancer Res.* 1999
- Cunha GR, Hayward SW, Wang YZ. Role of stroma in carcinogenesis of the prostate. *Differentiation.* 2002; 70:473–485. [PubMed: 12492490]
- Grossfeld G, Hayward S, Tlsty T. The role of stroma in prostatic carcinogenesis. *Endocrine-related ...* 1998
- Joesting M, Perrin S, Elenbaas B, Fawell S. Identification of SFRP1 as a candidate mediator of stromal-to-epithelial signaling in prostate cancer. *Cancer Res.* 2005
- Ao M, Franco O, Park D, Raman D, Williams K. Cross-talk between paracrine-acting cytokine and chemokine pathways promotes malignancy in benign human prostatic epithelium. *Cancer Res.* 2007
- He Y, Franco OE, Jiang M, Williams K, Love HD, Coleman IM, Nelson PS, Hayward SW. Tissue-specific consequences of cyclin D1 overexpression in prostate cancer progression. *Cancer Res.* 2007; 67:8188–8197. [PubMed: 17804732]
- Franco OE, Jiang M, Strand DW, Peacock J, Fernandez S, Jackson RS, Revelo MP, Bhowmick NA, Hayward SW. Altered TGF- Signaling in a Subpopulation of Human Stromal Cells Promotes Prostatic Carcinogenesis. *Cancer Res.* 2011; 71:1272–1281. [PubMed: 21303979]
- Orr B, Vanpoucke G, Grace O, Smith L. Expression of pleiotrophin in the prostate is androgen regulated and it functions as an autocrine regulator of mesenchyme and cancer associated fibroblasts and as a *The ...* 2011
- Orr B, Riddick A, Stewart G, Anderson R. Identification of stromally expressed molecules in the prostate by tag-profiling of cancer-associated fibroblasts, normal fibroblasts and fetal prostate. *Oncogene.* 2011

13. Vanpoucke G, Orr B, Grace C, Chan R, Ashley GR, Williams K, Franco OE, Hayward SW, Thomson AA. Transcriptional profiling of inductive mesenchyme to identify molecules involved in prostate development and disease. *Genome Biol.* 2007; 8:R213. [PubMed: 17922897]
14. Bhowmick NA, Neilson EG, Moses HL. Stromal fibroblasts in cancer initiation and progression. *Nature.* 2004; 432:332–337. [PubMed: 15549095]
15. Cheng N, Bhowmick N, Chytil A, Gorksa A. Loss of TGF- β type II receptor in fibroblasts promotes mammary carcinoma growth and invasion through upregulation of TGF- α -, MSP-and HGF-mediated signaling *Oncogene.* 2005
16. MacDougall J. Contributions of tumor and stromal matrix metalloproteinases to tumor progression, invasion and metastasis. *Cancer and Metastasis Reviews.* 1995
17. McCawley L. Matrix metalloproteinases: they're not just for matrix anymore! *Current opinion in cell biology.* 2001
18. Tuxhorn J, Ayala G. Reactive stroma in prostate cancer progression. *The Journal of urology.* 2001
19. Egberts F, Heinrich M, Jensen J. Cathepsin D is involved in the regulation of transglutaminase 1 and epidermal differentiation. *Journal of cell* 2004
20. Guicciardi M, Leist M. Lysosomes in cell death. *Oncogene.* 2004
21. CHEN S, ARANY I, APISARNTHANARAX N. Response of keratinocytes from normal and psoriatic epidermis to interferon- γ differs in the expression of zinc- α 2-glycoprotein and cathepsin D. *The FASEB Journal.* 2000
22. Laurent-Matha V. Catalytically inactive human cathepsin D triggers fibroblast invasive growth. *The Journal of Cell Biology.* 2005; 168:489–499. [PubMed: 15668295]
23. HARA I, MIYAKE H, YAMANAKA K, HARA S. Serum cathepsin D and its density in men with prostate cancer as new predictors of disease progression. *Oncology reports.* 2002
24. Rochefort H, Garcia M, Glondu M, Laurent V. Cathepsin D in breast cancer: mechanisms and clinical applications, a 1999 overview. *Clinica chimica acta.* 2000
25. Vetvicka V, Vetvickova J. Effect of procathepsin D and its activation peptide on prostate cancer cells. *Cancer letters.* 1998
26. Konno S, Cherry JP, Mordente JA, Chapman JR, Choudhury MS, Mallouh C, Tazaki H. Role of cathepsin D in prostatic cancer cell growth and its regulation by brefeldin A. *World J Urol.* 2001; 19:234–239. [PubMed: 11550780]
27. Morikawa W, Yamamoto K, Ishikawa S, Takemoto S, Ono M, Fukushi JI, Naito S, Nozaki C, Iwanaga S, Kuwano M. Angiostatin generation by cathepsin D secreted by human prostate carcinoma cells. *J. Biol. Chem.* 2000; 275:38912–38920. [PubMed: 10986284]
28. Tsukuba T, Okamoto K, Yasuda Y, Morikawa W, Nakanishi H, Yamamoto K. New functional aspects of cathepsin D and cathepsin E. *Mol. Cells.* 2000; 10:601–611. [PubMed: 11211863]
29. Hayward SW, Dahiya R, Cunha GR, Bartek J, Deshpande N, Narayan P. Establishment and characterization of an immortalized but non-transformed human prostate epithelial cell line: BPH-1. *In Vitro Cell. Dev. Biol. Anim.* 1995; 31:14–24. [PubMed: 7535634]
30. Hayward SW, Wang Y, Cao M, Hom YK, Zhang B, Grossfeld GD, Sudilovsky D, Cunha GR. Malignant transformation in a nontumorigenic human prostatic epithelial cell line. *Cancer Res.* 2001; 61:8135–8142. [PubMed: 11719442]
31. Williams K, Fernandez S, Stien X, Ishii K, Love HD, Lau Y-FC, Roberts RL, Hayward SW. Unopposed c-MYC expression in benign prostatic epithelium causes a cancer phenotype. *Prostate.* 2005; 63:369–384. [PubMed: 15937962]
32. Hayward SW, Haughney PC, Rosen MA, Greulich KM, Weier H-UG, Dahiya R, Cunha GR. Interactions between adult human prostatic epithelium and rat urogenital sinus mesenchyme in a tissue recombination model. *Differentiation.* 1998; 63:131–140. [PubMed: 9697307]
33. Hayward SW, Haughney PC, Lopes ES, Danielpour D, Cunha GR. The rat prostatic epithelial cell line NRP-152 can differentiate in vivo in response to its stromal environment. *Prostate.* 1999; 39:205–212. [PubMed: 10334110]
34. Reid WA, McGeachan K, Branch T, Gray HD, Thompson WD, Kay J. Immunolocalisation of aspartic proteinases in the developing human stomach. *J. Dev. Physiol.* 1989; 11:299–303. [PubMed: 2693525]

35. Weidner N, Folkman J, Pozza F. Tumor angiogenesis: a new significant and independent prognostic indicator in early-stage breast carcinoma. *Journal of the ...* 1992
36. Glondu M, Liaudet-Coopman E, Derocq D, Platet N, Rochefort H, Garcia M. Down-regulation of cathepsin-D expression by antisense gene transfer inhibits tumor growth and experimental lung metastasis of human breast cancer cells. *Oncogene*. 2002; 21:5127–5134. [PubMed: 12140763]
37. Nomura T, Katunuma N. Involvement of cathepsins in the invasion, metastasis and proliferation of cancer cells. *J. Med. Invest.* 2005; 52:1–9. [PubMed: 15751268]
38. Shen J, Person M, Zhu J, Abbruzzese J. Protein expression profiles in pancreatic adenocarcinoma compared with normal pancreatic tissue and tissue affected by pancreatitis as detected by two-dimensional *Cancer Res.* 2004
39. Tumminello FM, Leto G, Pizzolanti G, Candiloro V, Crescimanno M, Crosta L, Flandina C, Montalto G, Soresi M, Carroccio A, Bascone F, Ruggeri I, Ippolito S, Gebbia N. Cathepsin D, B and L circulating levels as prognostic markers of malignant progression. *Anticancer Res.* 1996; 16:2315–2319. [PubMed: 8694562]
40. Nadji M, Fresno M, Nassiri M, Conner G. Cathepsin D in host stromal cells, but not in tumor cells, is associated with aggressive behavior in node-negative breast cancer. *Human pathology.* 1996
41. Bacac M, Provero P, Mayran N, Stehle J-C, Fusco C, Stamenkovic I. A mouse stromal response to tumor invasion predicts prostate and breast cancer patient survival. *PLoS ONE.* 2006; 1:e32. [PubMed: 17183660]
42. Neuman E, Ladha M, Lin N. Cyclin D1 stimulation of estrogen receptor transcriptional activity independent of cdk4. ... and cellular biology. 1997
43. Lyons RM, Keski-Oja J, Moses HL. Proteolytic activation of latent transforming growth factor-beta from fibroblast-conditioned medium. *The Journal of Cell Biology.* 1988; 106:1659–1665. [PubMed: 2967299]
44. Phillips JL, Hayward SW, Wang Y, Vasselli J, Pavlovich C, Padilla-Nash H, Pezullo JR, Ghadimi BM, Grossfeld GD, Rivera A, Linehan WM, Cunha GR, Ried T. The consequences of chromosomal aneuploidy on gene expression profiles in a cell line model for prostate carcinogenesis. *Cancer Res.* 2001; 61:8143–8149. [PubMed: 11719443]
45. Reles A, Wen WH, Schmider A, Gee C, Runnebaum IB, Kilian U, Jones LA, El-Naggar A, Minguillon C, Schönborn I, Reich O, Kreienberg R, Lichtenegger W, Press MF. Correlation of p53 mutations with resistance to platinum-based chemotherapy and shortened survival in ovarian cancer. *Clin. Cancer Res.* 2001; 7:2984–2997. [PubMed: 11595686]
46. Ling V. Multidrug resistance: molecular mechanisms and clinical relevance. *Cancer chemotherapy and pharmacology.* 1997
47. Pérez-Tomás R. Multidrug resistance: retrospect and prospects in anti-cancer drug treatment. *Curr. Med. Chem.* 2006; 13:1859–1876. [PubMed: 16842198]
48. Qiu W, Hu M, Sridhar A, Opeskin K, Fox S, Shipitsin M, Trivett M, Thompson ER, Ramakrishna M, Goringe KL, Polyak K, Haviv I, Campbell IG. No evidence of clonal somatic genetic alterations in cancer-associated fibroblasts from human breast and ovarian carcinomas. *Nat Genet.* 2008; 40:650–655. [PubMed: 18408720]
49. Allinen M, Beroukhi R, Cai L, Brennan C. Molecular characterization of the tumor microenvironment in breast cancer. *Cancer Cell.* 2004

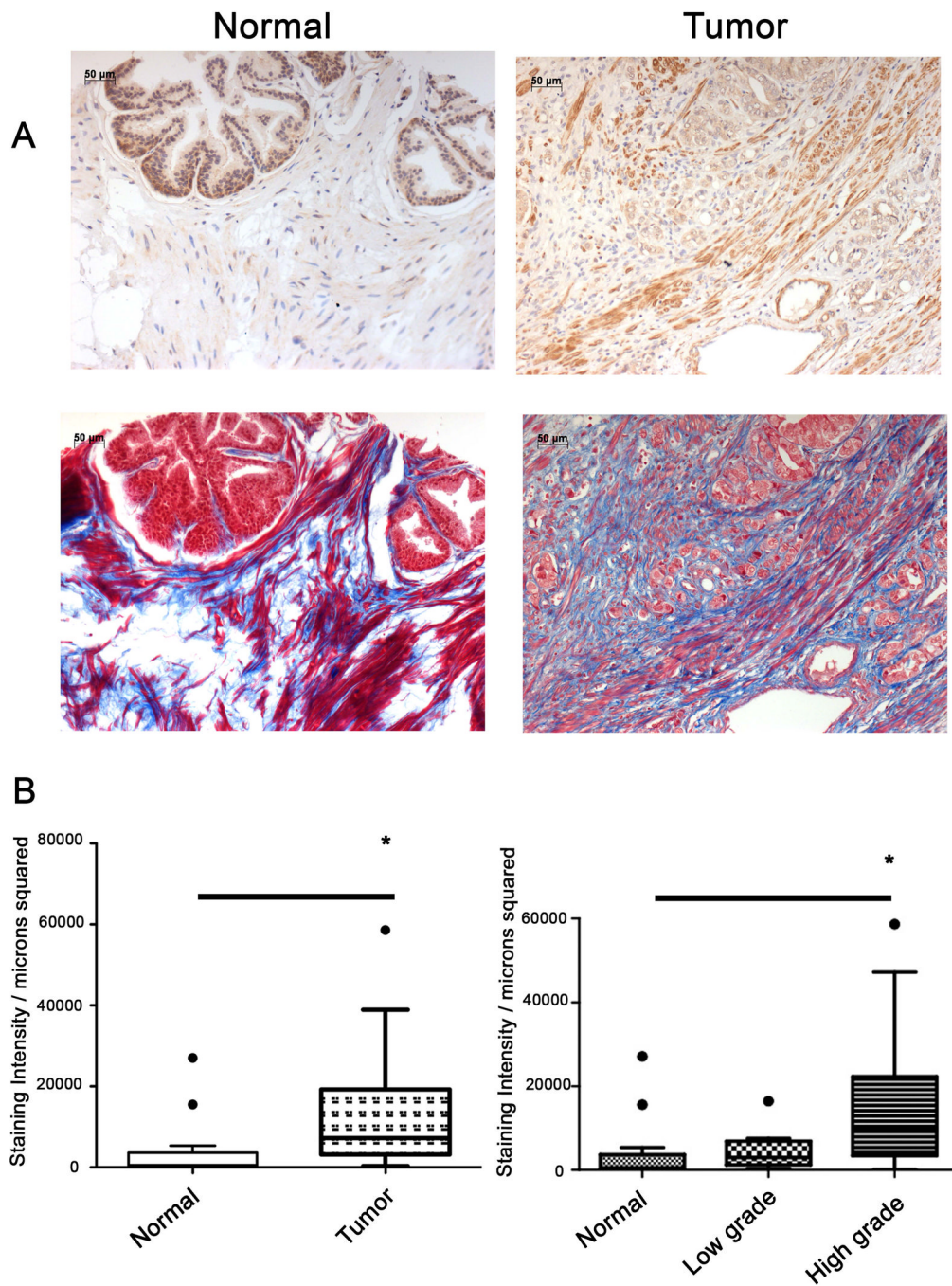


Figure 1. Cathepsin D is overexpressed in malignant prostate clinical samples

(A) Representative images from immunohistochemical (top) analysis of CathD expression in normal (left) $n = 18$ and tumor (right) $n = 30$ human prostate tissues. Representative images of Masson's tri-chrome staining (bottom) from normal (left) and tumor (right). Scale bar is equal to $50\mu\text{m}$. (B) Quantitation of CathD expression in the prostate comparing normal to malignant tissue. Data are presented as means \pm SD.

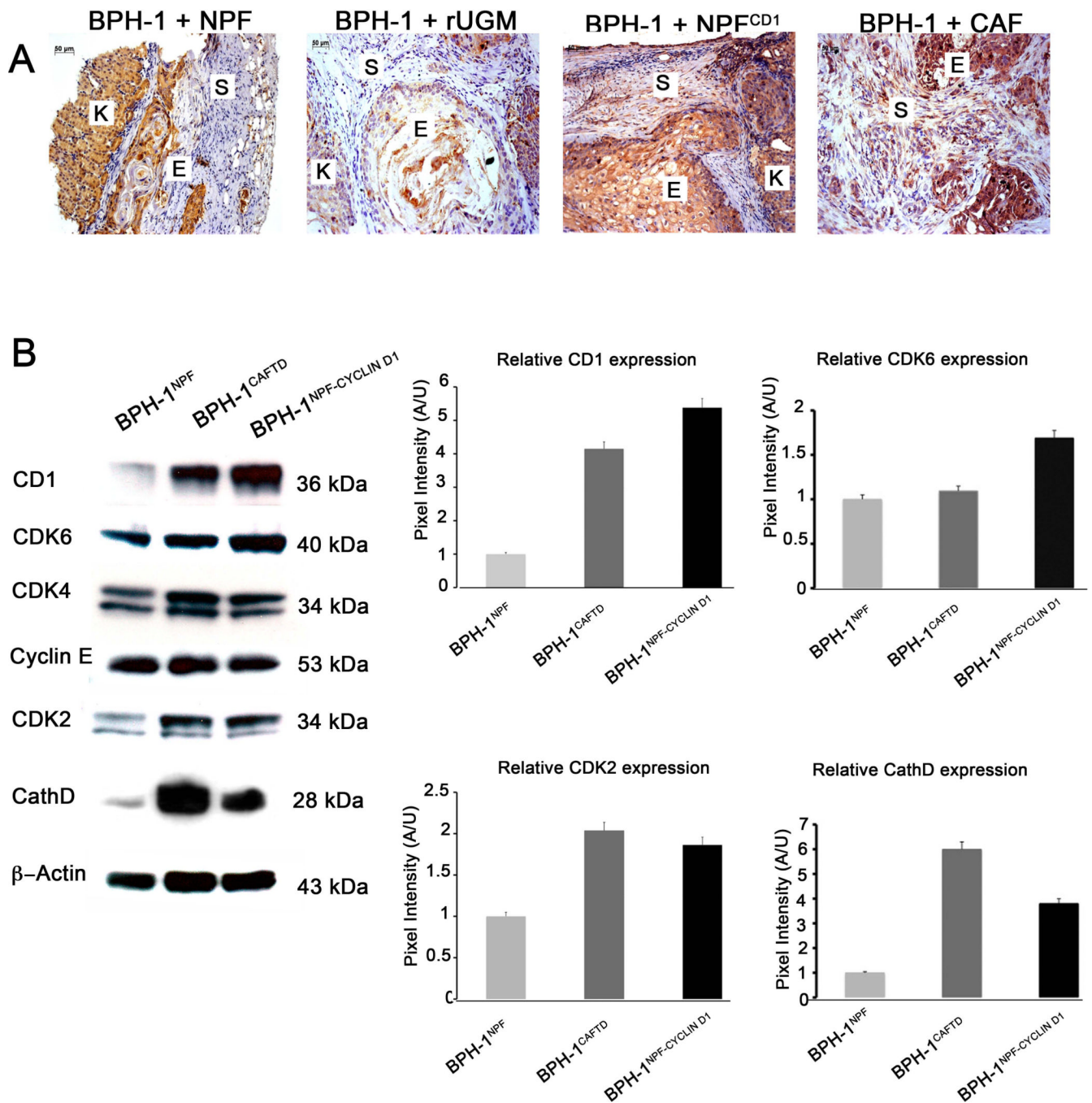


Figure 2. Evaluation of Cathepsin D as a paracrine mediator of neoplastic epithelial cell growth in tissue recombinants *in vivo*

(A) Immunohistochemical analysis of CathD expression in recombinations of 1) BPH-1 + NPF, 2) BPH-1 + rUGM, 3) BPH-1 + NPF^{CD1}, 4) BPH-1 + CAF. Scale bar is equal to 50µm (Letters K,S,E, refer to kidney, stroma, and epithelium). (B) Evaluation of densitometric analysis of cell cycle regulators and CathD in BPH-1^{NPF}, BPH-1^{CAFTD}, BPH-1^{NPFCD1} cells. Expression of Beta-actin was used for a loading control. Graphical representation of the mean ± SD of band intensities.

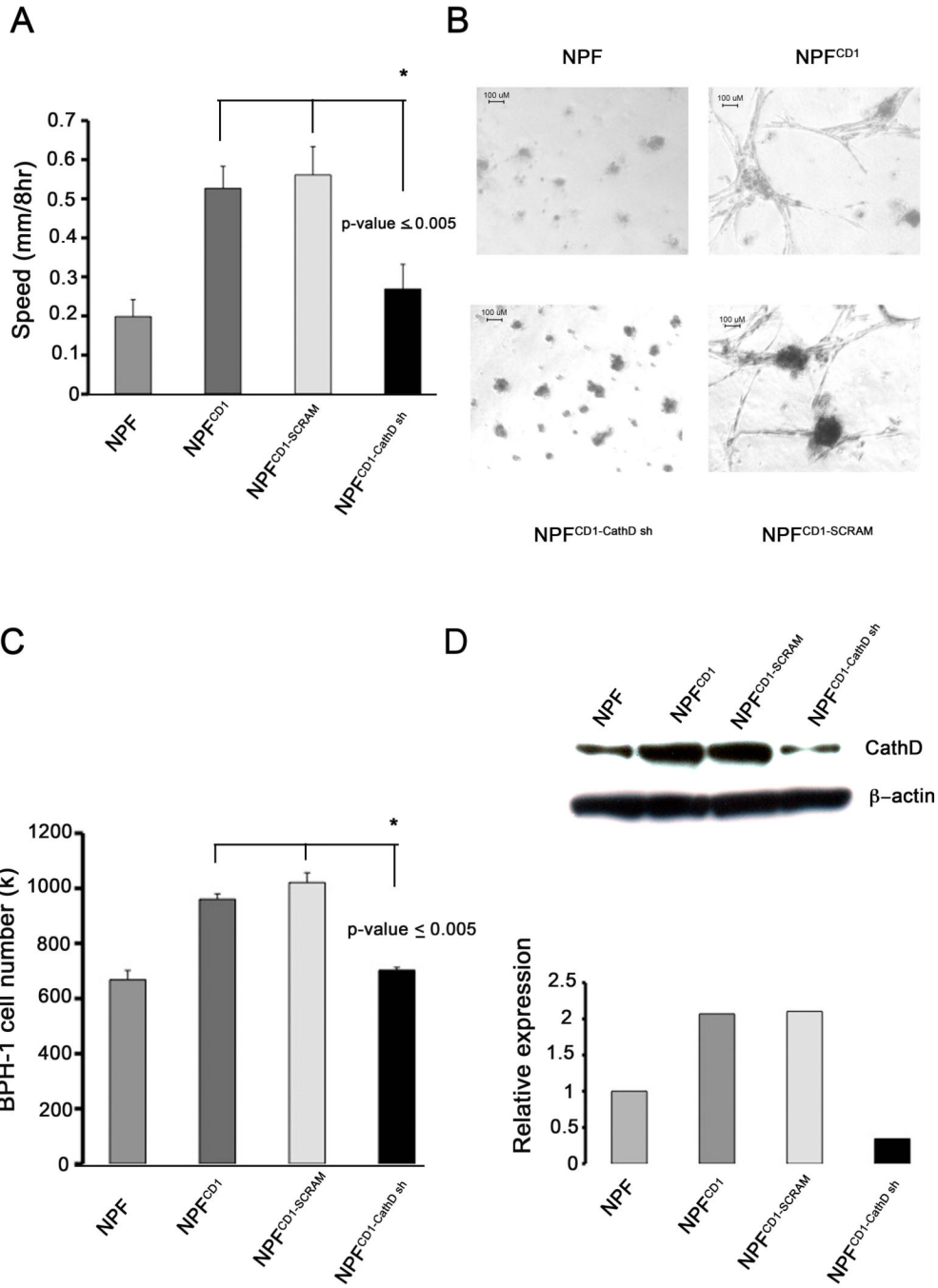


Figure 3. Cathepsin D is a critical mediator between BPH-1 cells and NPF^{CD1} *in vitro*
 (A) Wound healing assay. Confluent monolayers of NPF, NPF^{CD1}, NPF^{CD1}-control, NPF^{CD1}-CathD sh were scratched with a pipette tip. Bar graphs represent the mean ± SD of rate of wound closure over 8 hour period. Significance determined by ANOVA, p-value 0.005 n=3. (B) 3D outgrowth assays. NPF cell lines were embedded in matrigel and cultured for 14 days, scale bar = 100µm. Images taken at 10x (3B, b). (C) Evaluation of CathD as a paracrine mediator of growth. BPH-1 cells were treated with conditioned media collected from NPF cell lines for 3 days. Cell numbers were quantitated by direct counting, graphical representation of the mean ± SD of the experiment is shown, significance determined by ANOVA p-value 0.005 n=3. (D) Western blot confirming knockdown of CathD in NPF,

NPF^{CD1}, NPF^{CD1-control}, NPF^{CD1-CathD sh} cells (Top). Densitometric analysis of band intensities performed to determine knockdown efficiency (Bottom).

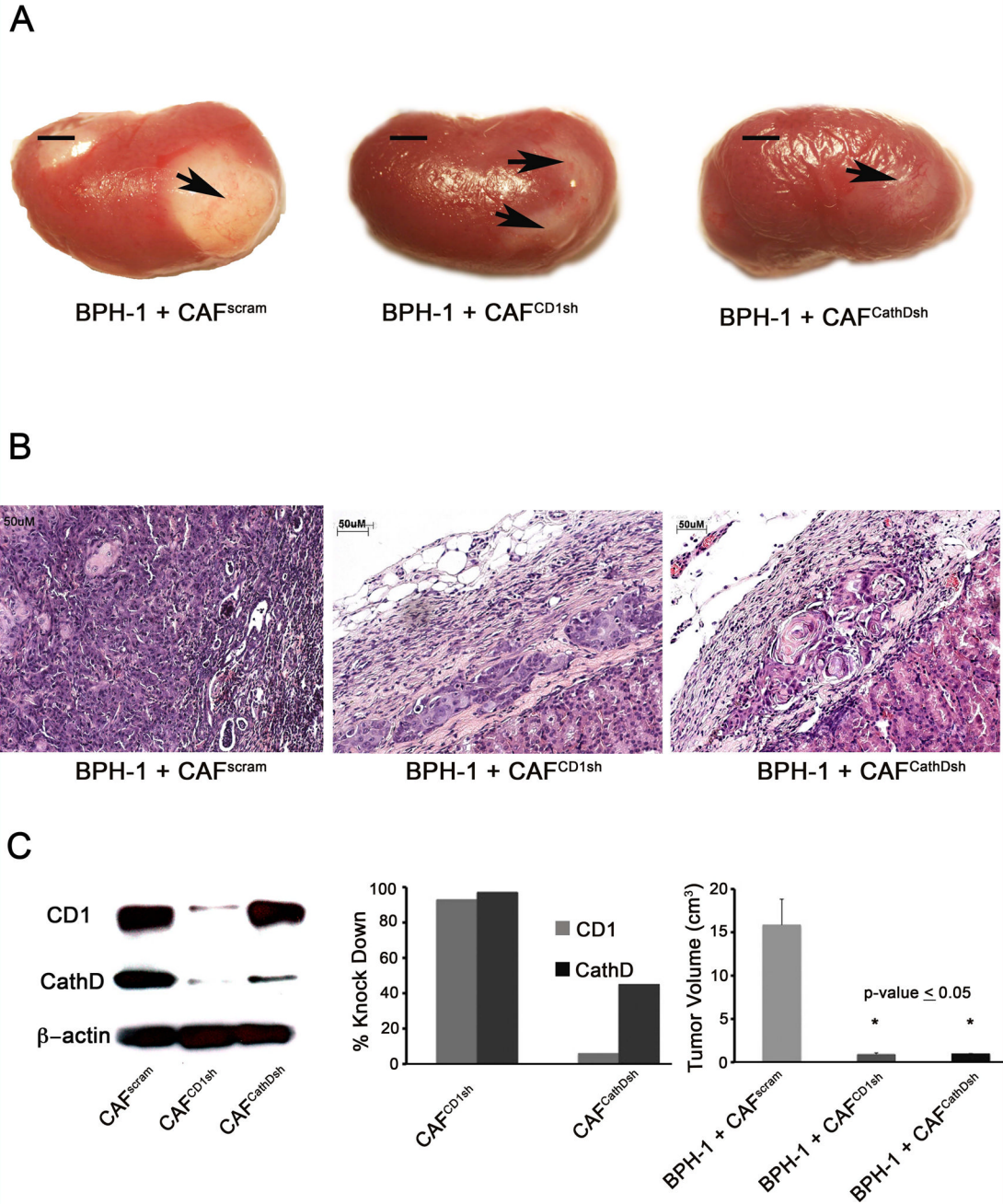


Figure 4. Cyclin D1 and Cathepsin D are required for CAF induced tumorigenicity *in vivo* (A) Gross morphology of 2 month grafts of BPH-1 + CAF^{PSR}, BPH-1 + CAF^{CD1sh}, and BPH-1 + CAF^{CathDsh}, scale bar equal to 5cm. (B) H&E staining of BPH-1 + CAF^{PSR}, CAF^{CD1sh}, or CAF^{CathDsh}. BPH-1 + CAF^{PSR} recombinants formed adenosquamous carcinoma as previously described. Scale bar equal to 50μm (C) Western blot confirming knockdown of CD1 and CathD in CAFs (left). Knockdown efficiency determined by performing densitometric analysis of western blot represented by bar graph (middle). Quantitation of tumor volume of 2 month grafts of BPH-1 + CAF^{PSR}, BPH-1 + CAF^{CD1sh}, and BPH-1 + CAF^{CathDsh} (right), graphical representation of the mean ± SD of the grafts is shown in n=6. Significance determined by ANOVA, p-value 0.05.

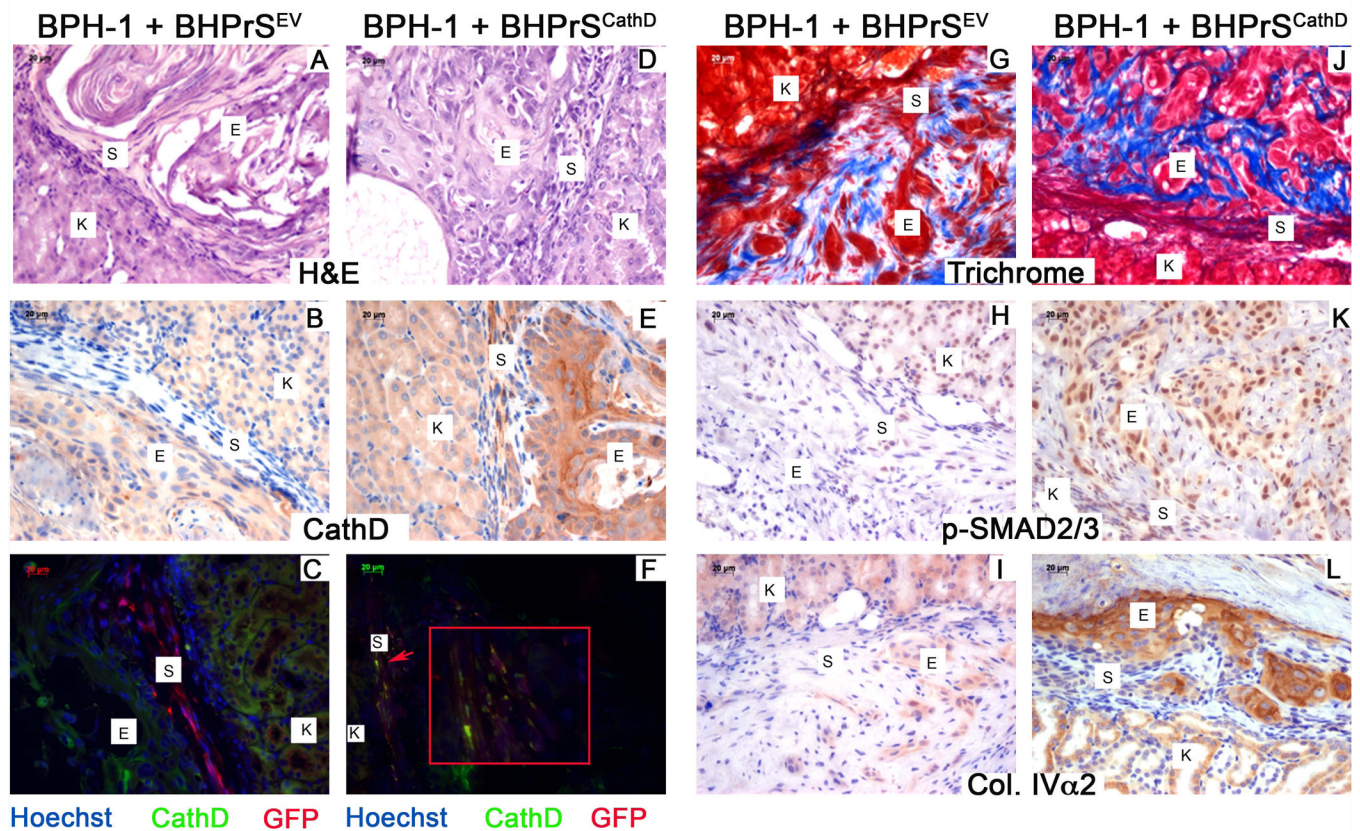


Figure 5. Overexpression of Cathepsin D induces a malignant transformation through activation of TGF β signaling

(A) Characterization of CathD overexpressing grafts. H&E staining (top) of BPH-1 + BHPPrS^{EV} and BPH-1 + BHPPrS^{CathD}. Recombinations of BPH-1 + BHPPrS^{CathD}, produced malignant transformations. IHC for CathD (middle) strong expression visible in the stroma of recombinations of BPH-1 + BHPPrS^{CathD}. Immunofluorescence for CathD (green) and GFP (red) show co-localization for GFP and CathD (yellow) in recombinations of BPH-1 + BHPPrS^{CathD}. (B) Masson's trichrome staining (top) of recombinations of BPH-1 + BHPPrS^{EV} and BPH-1 + BHPPrS^{CathD}. IHC for p-SMAD2/3 (middle) and Collagen IV α 2 (lower) in recombinations of BPH-1 + BHPPrS^{EV} and BPH-1 + BHPPrS^{CathD}. Scale bar equal to 20 μ m.